Surface-Wave Tomography at Mining Sites - A Case Study from Central Sweden

We_25th_B08

Surface-Wave Tomography at Mining Sites - A Case Study from Central Sweden

M. Papadopoulou [1]*, F. Da Col [1], L.V. Socco [1], S. Hu [2], E. Bäckström [3], M. Schön [3], P. Marsden [3], A. Malehmir [4]

[1] Politecnico di Torino; [2] Tongji University; [3] Nordic Iron Ore AB; [4] Uppsala University

Summary

In mineral exploration, a detailed description of the near-surface is important when seismic reflection is applied, because the heterogeneity of the shallow layers can influence the imaging of deeper targets. The use of surface waves can provide valuable information about the shallow subsurface but multichannel methods might be limited by the existence of lateral variations in the subsurface. On the contrary, surface-wave tomography has the potential to locate more accurately subsurface heterogeneities and lateral variations without lacking penetration depth. We apply surface-wave tomography on the mining site of Blötberget (Ludvika Mines, Sweden). A checkerboard test provides information about the resolution and is used for the parameterization of the initial model for the tomographic inversion. The results provide a detailed description of the shallow subsurface, showing the potential of using surface-wave tomography in seismic exploration, also for challenging data from mining sites.

Introduction

Surface-wave (SW) methods are based on the analysis of the geometric dispersion of SW, which is extracted from seismic data as the relationship of SW phase velocity and frequency (dispersion curve or DC). In hydrocarbon exploration, SW are used to provide information for the shallow subsurface and estimate static corrections, which are necessary to remove the effect of the shallow, highly heterogeneous low-velocity overburden (weathering layer) enabling improved imaging of the deeper exploration targets. As seismic reflection is becoming popular also in the mineral exploration industry (Malehmir et al., 2012), the need to adapt SW methods to characterize the near surface in hard rock settings increases. However, several challenges related to crystalline-rock environment such as possible lateral heterogeneities such as deformation and fracturing in stiff rocks, man-made structures, mining tunnels and sometimes voids produced during block-caving mining should be addressed.

Multichannel SW analysis, which is mainly applied in exploration, may not be effective in delineating such sharp lateral variations. In the traditional SW methods, the DCs are estimated for a window of receivers and represent the average properties of the subsurface below the window. If a small velocity anomaly exists below the window, its effect on the inversion result might be smoothened. On contrary, SW tomography, which is the most common method in global seismology, measures the path-average dispersion characteristics between all possible couples of receivers and inverts local 1D velocity models with a tomographic algorithm. Therefore, because there is redundancy in the information in SW tomography, it has the potential to locate more accurately subsurface heterogeneities and lateral variations without lacking penetration depth. Even though most applications of this method focus on regional or global scale, active SW tomography has been implemented and applied for the characterization of the near-surface at exploration scale (Socco et al., 2014).

Here we apply SW tomography on a legacy active-source seismic 2D dataset from a mining site in Sweden. The data were pre-processed to obtain good-quality path-average dispersion curves. Several checkerboard tests with different block sizes were run to analyse the available resolution and parametrize the initial model for the tomographic inversion.

Method

The dispersion information between two receivers is estimated through the two-station method (Yao et al., 2008). The phase velocity between two receivers is estimated by cross-correlating the signals of the two receivers and a common, in-line source. The cross-correlation matrix can be used to estimate the average slowness dispersion curves along the path between the two receivers. Since recorded data from different shots are available, their spectra are stacked for the same receiver couples to increase S/N. This process is repeated for different couples of receivers until the data coverage of the volume under investigation is satisfactory.

The resolution achievable with the inversion is assessed by the means of conventional checkerboard tests. Since the acquisition is 2D, the test has the special form of a “zebra” test as described in Da Col (2014). According to the test, a 1D-VS model is perturbed to create a canvas of alternating positively and negatively (similar to the fur of a zebra) perturbed stripes. The dimensions of the stripes are related to the size of the features to be mapped with the tomography. Synthetic dispersion curves are computed with a forward modelling code for the same source/receiver geometry as the real data. The inversion result is compared to the true model and the accuracy with which the stripes are detected indicates the resolution.

The retrieved path-averaged dispersion data are inverted with a tomographic inversion method described in Boiero (2009). It is a damped least-squared inversion method that is computationally efficient and inverts directly for 1D VS models. If a priori information is available, it is included in the form of lateral and/or vertical constraints in the model parameters. The initial model for the inversion is parametrized according to the results of the zebra test.

Field data

The method was applied to a legacy dataset from Blötberget of Ludvika Mines in central Sweden. The seismic data were acquired in 2016 under a seismic reflection study (a description of the site and acquisition setup exists in Markovic et al., 2018). We focus our analysis on the northwestern portion of the profile (281 receivers and shots marked in black in Figure 1a), where it is known from previous studies that possibly some local heterogeneities exist.

Previous studies (Papadopoulou et al., 2018) have shown that processing this dataset for SW is challenging because the data suffer from low S/N. To improve the retrieval of the fundamental mode of Rayleigh waves, shot gathers were muted. To ensure coverage, different receiver couples for the two-station method were chosen at different locations along the profile ensuring sufficient path overlap. The phase-velocity spectrum computed for each couple was stacked for all available shots to improve S/N. Moreover, for SW, low frequencies (longer wavelengths) propagate at greater depths. Thus, the receiver couples were chosen having variable separations to improve coverage in wavelength and therefore at depth. Narrow trace separation includes shorter wavelengths allowing the retrieval of the information of the shallow part of the subsurface while larger separation is required for longer wavelengths and is thus necessary to investigate greater depths. According to these criteria, 109 average dispersion curves were picked (Figure 1b).

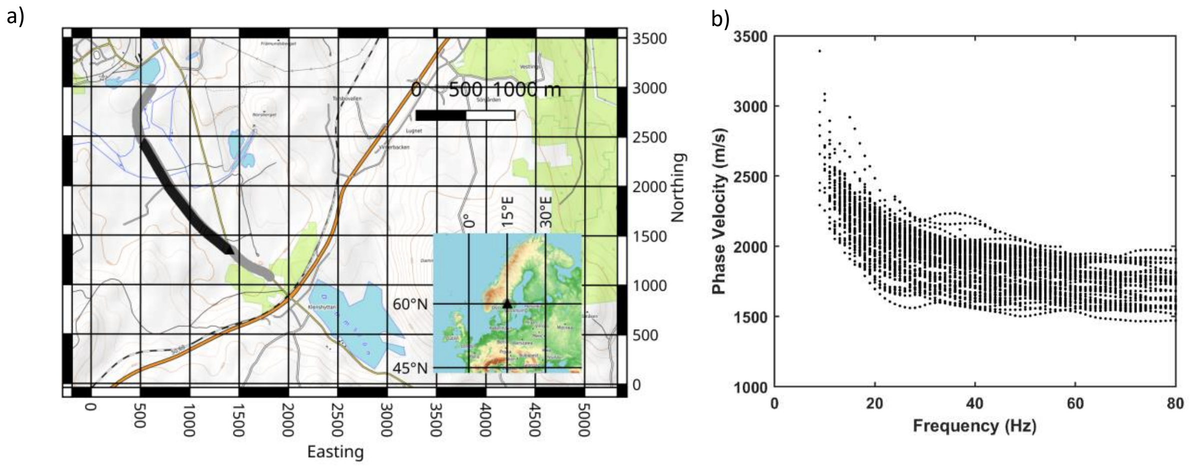

Figure 1 *a) The 2016 seismic data acquisition setup highlighted in grey. The black line corresponds to the positions of the 281 receivers and shots selected for processing. Easting and Northing Coordinates are relative to point (504000,6661500) expressed in UTM33V. b) Average phase velocity dispersion curves picked for the same receiver couples for stacked shots and muted shot gathers. The frequency band and phase velocity range of each curve depends on the subsurface properties along the two receivers and their separation. The curves are homogeneous and show high values of phase velocity, related to the presence of a stiff rock.*

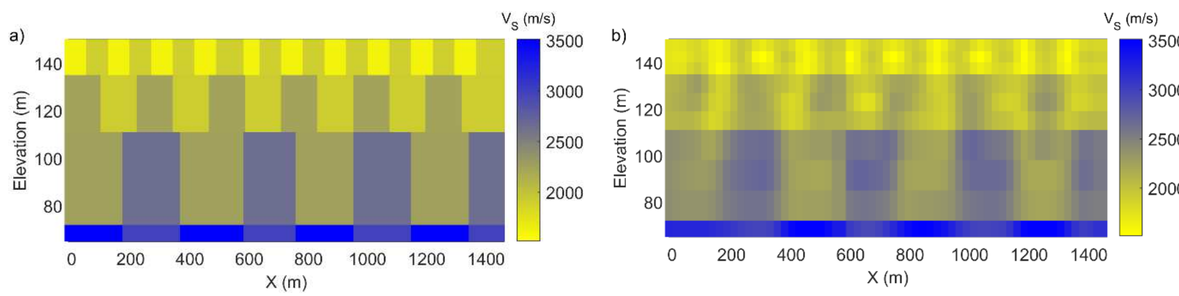

Figure 2 *a) "Zebra" model resulting from perturbing by ±8% a synthetic layered VS mode and by increasing the stripe size with depth. b) Result of the tomographic inversion of the "zebra" mode after 30 iterations. The velocity anomalies can be adequately estimated.*

To create the synthetic "zebra" model, we started from a 1D-VS model, which was obtained by inverting the average of all the dispersion curves. To implement the zebra test, we first discretized this 1D model to thin (5 m) layers and the velocity was perturbed to create velocity anomalies, the zebra stripes, with size 75x15 m. According to Pan et al. (2016) the size of the velocity stripes is an important parameter that should be carefully chosen according to the type of SW, the separation of the receivers, the data quality and the frequency band. Following their strategy, we ran two additional zebra tests with different stripe sizes (120x24 m and 170x40 m) and every time the velocity was perturbed by ±8%. The thickness of the model layers was different every time (8 m for the second and 13 m for the third test). At each zebra test, the synthetic dispersion curves were inverted using the tomographic code described in the method section. The results showed that the smaller sizes could be mapped in the shallow layers, until a threshold value of depth below which larger stripes could only be resolved.

After running the three zebra tests, all the results were combined to one zebra model for which the stripe size increases with depth (Figure 2a). The result after 30 iterations (Figure 2b) suggests that the velocity variations at different depths can be resolved with different resolutions.

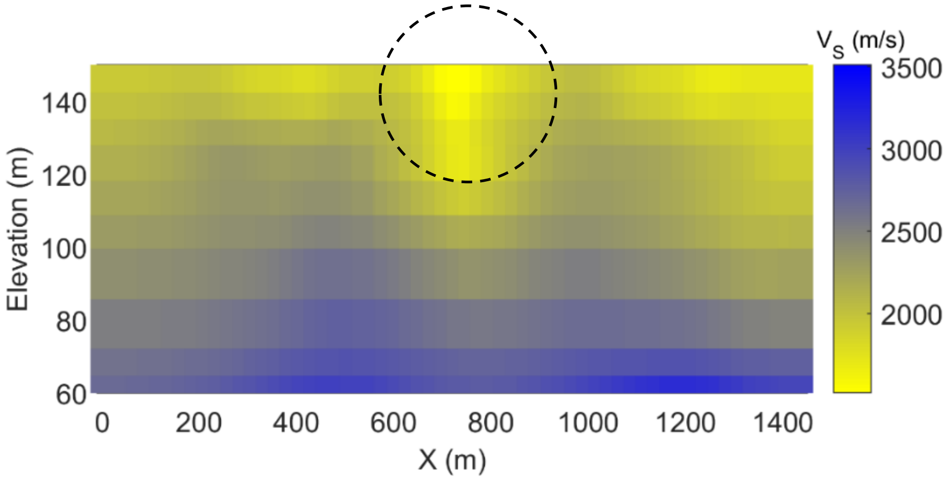

Figure 3 *Inversion result of the experimental data. High VS values are estimated, indicating the presence of stiff tock. The black dashed circle indicates a strong velocity anomaly in the centre of the line, probably caused by a local discontinuity.*

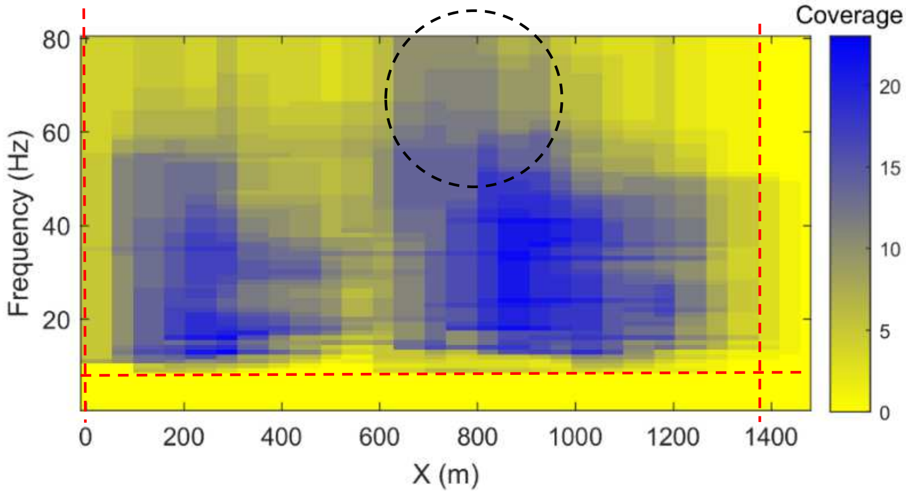

Figure 4*. Data coverage along the line. The coverage is computed as the number of dispersion curves picked for paths crossing the 1D model positions. The red dashed lines represent the positions and frequencies at which the dispersion curves provide adequate illumination (coverage > 0). The plot indicates that the location of velocity anomaly (black dashed circle) is illuminated by the data.*

The experimental data were inverted starting from 60 homogeneous 1D models along the receiver line, discretized with the same layer thicknesses as in the "zebra" model inversion and with VS=3250 m/s, ρ=2000 kg/m^3 and υ=0.3. A spatial velocity constraint in the layer velocity was applied based on prior knowledge of the site (Papadopoulou et al., 2018) and nine iterations were performed. The result (Figure 3) shows an increase of VS with depth and reaches a value of approximately 3000 m/s at the bedrock, the position of which varies among the different models. In the central part of the line a strong velocity anomaly (marked with the dashed circle in Figure 3) that can be attributed to a local discontinuity, is present at shallow depths. The data coverage for all frequency components of the dispersion curves is computed as the number of paths that intersect the positions of the 1D models and is plotted for all the positions (Figure 4). The area where the coverage is greater than 1 is marked with the red dashed lines. According to this figure, positions at offset lower than 1400 m, including the position of the strong energy anomaly indicated by the black circle, are illuminated by the data at a wide frequency band, increasing the confidence of the result.

Conclusions

The SW tomography provided a VS model, which is encouraging and may provide new information on a major structure intersecting the profile. We conclude that surface-wave tomography is capable to provide a good estimation of the shear-wave velocity also for challenging data from mining sites. Since the data suffer from low S/N, muting the raw data to isolate the fundamental mode of Rayleigh waves from body waves and recorded noise is recommended to improve the quality of the picked dispersion curves. The 2D checkerboard test can be used to assess the resolution of the inversion at a given model parameterization. Coverage provides information to assess the reliability of the results.

Acknowledgements

We thank Uppsala University and Nordic Iron Ore AB (NIO) for providing access to the data in the framework of Smart Exploration project. Smart Exploration has received funding from the European Union's Horizon 2020 research and innovation programme under grant agreement No. 775971.

References

Boiero, D. [2009]. Surface Wave Analysis for Building Shear Wave Velocity Models. Ph.D. Thesis.

Da Col, F. [2013] Surface Wave Tomography at Exploration Scale. *MSc Thesis*.

Malehmir, A., Durrheim, R., Bellefleur, G., Urosevic, M., Juhlin, C., White, D., Milkereit, B., and G. Campbell. [2012]. Seismic methods in mineral exploration and mine planning: A general overview of past and present case histories and a look into the future. *Geophysics*, 77, WC173–WC190. DOI: 10.1190/GEO2012-0028.1.

Markovic, M., Maries, G., Malehmir, A., Bäckström, E., Schön, M., Jakobsson, J. and P. Marsden. [2018] Deep Targeting Iron-Oxide Mineralization Using Reflection Seismic Method: A Case Study from the Ludvika Mines Of Sweden. *EAGE Near Surface Geoscience Conference & Exhibition 2018, Porto, Portugal*. DOI: 10.3997/2214-4609.201802702.

Pan, Y., Xia, J., Xu, Y., Gao, L. and Z. Xu. [2016] Love-wave waveform inversion in time domain for shallow shear-wave velocity. *Geophysics, 81, 2*. DOI: 10.1190/GEO2014-0225.1.

Papadopoulou, M., Da Col, F., Socco, L.V., Bäckström, E., Schön, M., Marsden P. and A. Malehmir. [2018] Application of Surface-Wave Analysis for Mineral Exploration: A Case Study from Central Sweden. *EAGE Near Surface Geoscience Conference & Exhibition 2018, Porto, Portugal*. DOI: 10.3997/2214-4609.201802704.

Socco, L.V., Boiero, D., Bergamo, P., Garofalo, F., Yao, H., Van Der Hilst, R.D. and F. Da Col. [2014] Surface wave tomography to retrieve near surface velocity models. *SEG Technical Program Expanded Abstracts 2014*, 2013-2018. http://dx.doi.org/10.1190/segam2014-1278.1.

Yao, H., van der Hilst, R.D., de Hoop, M.V. [2006]. Surface-wave array tomography in SE Tibet from ambient seismic noise and two-station analysis – I. *Geophysical Journal International*,166(2), 732-744. DOI: 10.1111/j.1365-246X.2006.03028.x.